

# Low- and High-Energy Expansion of Heavy-Quark Correlators at Next-To-Next-To-Leading Order

A. Maier<sup>a</sup>, P. Marquard<sup>b</sup>

<sup>a</sup>*INFN, Sezione di Torino & Dipartimento di Fisica Teorica, Università di Torino,  
10125 Torino, Italy*

<sup>b</sup>*Institut für Theoretische Teilchenphysik,  
Karlsruhe Institute of Technology (KIT), 76128 Karlsruhe, Germany*

---

## Abstract

We calculate three-loop corrections to correlation functions of heavy-quark currents in the low- and high-energy regions. We present 30 coefficients both in the low-energy and the high-energy expansion of the scalar and the vector correlator with non-diagonal flavour structure. In addition we compute 30 coefficients in the high-energy expansion of the diagonal vector, axial-vector, scalar and pseudo-scalar correlators. Possible applications of our new results are improvements of lattice-based quark-mass determinations and the approximate reconstruction of the full momentum dependence of the correlators.

*Key words:* Perturbative calculations, Quantum Chromodynamics, Heavy Quarks  
*PACS:*

---

## 1 Introduction

The precise determination of the fundamental parameters of the Standard Model (SM) is of utmost importance to pin down the fundamental interactions of the elementary particles and to establish deviations from the SM. Three especially interesting parameters, namely the strong coupling constant and the masses of charm and bottom quarks, can be determined with high accuracy from correlators of heavy-quark currents by comparing their moments with experimental data using sum rules [1,2]. Conventionally, moments from

the low-energy expansion have been used for this purpose [3–8], but also methods relying on high-energy moments have been shown to yield quite accurate results [9].

As an alternative to experimental data also lattice simulations can be used in order to compute moments of two-point functions. Thanks to significant improvements in the last years results can be obtained not only for the charm-quark mass and the strong coupling constant [10], but also for the bottom-quark mass [11].

Aside from these determinations, quark-current correlators have a number of additional phenomenological applications. Two examples are the sum-rule determinations of heavy-meson decay constants and  $\alpha_s(m_\tau)$  (for recent works see e.g. Refs [12–15]). While the former requires – among other ingredients – the low-energy expansion of the respective correlator, the latter uses the absorptive part above the production threshold.

In this work we consider correlators of quark currents with various different Lorentz structures. Furthermore we distinguish between diagonal and non-diagonal correlators. The diagonal correlators are defined through

$$\Pi_{\text{D}}^X(q) = i \int e^{iqx} \langle 0 | J^X(x) J^X(0) | 0 \rangle dx, \quad (1)$$

with the currents  $J^X(x)$  given by

$$J^X(x) = \bar{\psi}(x) \Gamma^X \psi(x). \quad (2)$$

The non-diagonal correlators are defined in analogy by

$$\Pi_{\text{ND}}^X(q) = i \int e^{iqx} \langle 0 | j^X(x) j^X(0) | 0 \rangle dx, \quad (3)$$

with the currents  $j^X(x)$  given by

$$j^X(x) = \bar{\psi}(x) \Gamma^X \chi(x). \quad (4)$$

Here  $\psi$  denotes a heavy quark while  $\chi$  stands for a massless one. The scalar, pseudo-scalar, vector and axial-vector currents are defined through the Dirac structures  $\Gamma^X = 1, i\gamma_5, \gamma_\mu, \gamma_\mu\gamma_5$  ( $X = s, p, v, a$ ), respectively. Note that in the case of the non-diagonal correlators  $\Pi_{\text{ND}}^s = \Pi_{\text{ND}}^p$  and  $\Pi_{\text{ND}}^v = \Pi_{\text{ND}}^a$  hold.

For the determination of the quark masses from experimental data only the diagonal vector correlator  $\Pi_{\text{D}}^v$  can be used while it is in principle possible to use all diagonal and non-diagonal correlators in combination with lattice simulations.

Current-current correlators have already been extensively studied in the literature. The two-loop corrections to the diagonal vector correlator have been

calculated in [16], the corresponding corrections for the non-diagonal one in [17]. At three loops the leading terms of the low- and high-energy expansion have been determined in [18,19]. For the diagonal correlators many terms in the low-energy expansion have been computed in [20,21]. At four loops the leading terms in the low-energy expansion of various currents have been calculated in [22,23,4,24,25]. In the high-energy region the expansion at four-loop order has been obtained in [26]. In [27] effects of a second massive quark have been taken into account at three-loop order. Collecting the available information for the correlators at three and four loops, the full momentum dependence has been approximated using Padé approximations and Mellin-Barnes inspired methods [28,18,29–32]. In this paper we complete the calculation of the low- and high-energy expansion of diagonal and non-diagonal heavy-quark correlators using an improved method for the calculation.

In Section 2 we present the details of the calculation. In Section 3 we present explicit results for the non-diagonal vector correlator in numerical form and discuss the convergence of the expansions. The analytical results for all correlators can be found on the web page

<http://www-ttp.particle.uni-karlsruhe.de/Progdata/ttp11/ttp11-25/>.

## 2 Details of the calculation

The calculation is organized as follows. The diagrams are generated using `qgraf` [33] and are subsequently mapped onto a small set of 11 topologies using `q2e` and `exp` [34]. After the application of suitable projectors the resulting scalar integrals are reduced to master integrals using integration-by-parts identities [35,36] implemented in the program `Crusher` [37]. The resulting expression which still contains the full dependence on both the external momentum square  $q^2$  and the heavy-quark mass  $m$  is then – lacking an analytical result for the master integrals – expanded in the energy region of interest as explained in more detail below. The expanded master integrals are combined in a `FORM` [38] program in order to obtain the final expressions valid in either the low-energy or the high-energy region.

The coupling constant  $\alpha_s$  is renormalized in the  $\overline{\text{MS}}$  scheme while for the renormalization of the heavy-quark mass  $m$  we employ both the  $\overline{\text{MS}}$  and the on-shell scheme. In the following we concentrate on the renormalization in the  $\overline{\text{MS}}$  scheme, the results for the on-shell scheme can be found on the web page mentioned above. For the overall normalization we employ  $\Pi^X(0) = 0$  with  $X \in v, a, s, p$ .

Let us now have a closer look at the technical details of the expansion of the master integrals. The starting point for the calculation of the expansion is a

suitable differential equation, which can easily be obtained from the master formula [39–41]

$$\mathcal{D}_i M_i(q^2, m^2) = 2 \left( q^2 \frac{\partial}{\partial q^2} + m^2 \frac{\partial}{\partial m^2} \right) M_i(q^2, m^2), \quad (5)$$

where  $\mathcal{D}_i$  is the mass dimension of the integral  $M_i(q^2, m^2)$ . The derivative with respect to  $m^2$  can be performed resulting in a differential equation with respect to  $q^2$  for the integral  $M_i(q^2, m^2)$ . The expansion in  $z = q^2/m^2$  can now be obtained by inserting a suitable ansatz, e.g.

$$M_i(q^2, m^2) = m^{\mathcal{D}_i} \sum_{k=0}^{\infty} A_{i,k} z^k \quad (6)$$

into the differential equation and solving the resulting linear system of equations for the coefficients  $A_{i,k}$ . Ansatz (6) is sufficient to obtain the low-energy expansion for the non-diagonal correlators. The only further input needed is the value of the integral for  $z = 0$ , which corresponds to the initial condition of the differential equation. In the case of the high-energy expansion ansatz (6) is not sufficient<sup>1</sup> but one has to use an ansatz of the form

$$M_i(q^2, m^2) = m^{\mathcal{D}_i} \sum_{k=k_0}^{\infty} \left( A_{i,k} + A_{i,k}^{(\epsilon)} (-z)^{-\epsilon} + A_{i,k}^{(2\epsilon)} (-z)^{-2\epsilon} + A_{i,k}^{(3\epsilon)} (-z)^{-3\epsilon} \right) z^{-k} \quad (7)$$

instead. The lower limit  $k_0$  and the initial conditions  $A_{i,k_0}$ ,  $A_{i,k_0}^{(l\epsilon)}$ ,  $l = 1, 2, 3$  can be determined from the leading terms of the asymptotic expansion for  $z \rightarrow -\infty$ . Generally, these leading terms consist of products of massive vacuum diagrams and massless propagators with a total number of three loops in each product. The coefficients  $A_{i,k_0}^{(l\epsilon)}$  are given by the products of propagators with a total of  $l$  loops and vacuum diagrams with  $3 - l$  loops. Consequently,  $A_{i,k_0}$  consists of the products without any massless propagators. The diagrams contributing to the initial conditions are shown in Fig. 1; in order to obtain dimensionless coefficients  $A_{i,k_0}$ ,  $A_{i,k_0}^{(l\epsilon)}$  we set  $-q^2 = m^2 = 1$  in those diagrams.

It should be noted that in practice it is convenient to just use a small enough universal value for  $k_0$  instead of carefully deriving it separately for each single master integral from the respective asymptotic expansion. Furthermore, most of the coefficients  $A_{i,k_0}$ ,  $A_{i,k_0}^{(l\epsilon)}$  are already determined by the linear system of equations and only a few remaining ones have to be determined through asymptotic expansion. The considerable freedom in the choice of the initial conditions also implies that the set of contributing diagrams shown in Fig. 1 is by no means unique.

<sup>1</sup> An extension is also necessary for the low-energy expansion of the diagonal correlators as discussed in detail in Ref. [21].



Larin [42] for the so-called singlet diagrams with exactly one  $\gamma_5$  in a fermion trace and a naïvely anticommuting  $\gamma_5$  for all other diagrams. In order to present only anomaly-free quantities the axial-vector correlator is computed for a quark isospin doublet  $(\psi, \chi)$  like in Ref. [21].

### 3 Results

Since the full results are very lengthy we present only the numerical results for the non-diagonal vector correlator. The analytical results for all correlators can be found on the web page

<http://www-ttp.particle.uni-karlsruhe.de/Progdata/ttp11/ttp11-25/>.

The expansion has been performed in  $z = q^2/m^2$ . The results for the first 6 low-energy and 8 high-energy coefficients agree with Ref. [19].

The vector correlator can be written as

$$\Pi_{\text{ND},v}^{\mu\nu}(q^2) = (-q^2 g^{\mu\nu} + q^\mu q^\nu) \Pi_{\text{ND}}^v(q^2) + q^\mu q^\nu \Pi_{\text{ND},L}^v, \quad (9)$$

We present only the results for the transversal part of the vector correlator, the longitudinal part can be obtained from the results for the scalar one. In the following we set the renormalization scale  $\mu = m$  during the numerical evaluation.

In Table 1 we present the numerical results for the low-energy expansion of the non-diagonal vector correlator which is decomposed according to

$$\begin{aligned} \Pi_{\text{ND}}^v = & \frac{3}{16\pi^2} \sum_{n>0} \left( \bar{C}_n^{(0),v} + \frac{\alpha_s}{\pi} \bar{C}_n^{(1),v} \right. \\ & \left. + \left( \frac{\alpha_s}{\pi} \right)^2 \left( \bar{C}_n^{(2),v}[1] + n_h \bar{C}_n^{(2),v}[n_h] + n_l \bar{C}_n^{(2),v}[n_l] \right) \right) z^n. \end{aligned} \quad (10)$$

$\bar{C}_n^{(2),v}[n_h]$  and  $\bar{C}_n^{(2),v}[n_l]$  contain the contributions from closed heavy and light quark loops, respectively.

The results for the high-energy expansion shown in Tables 2–4 are more complicated due to logarithmic contributions. Since the correlator is known analytically up to two loops we present only the results for the three-loop contri-

bution. It is decomposed as

$$\begin{aligned} \Pi_{\text{ND}}^{v,3\text{-loop}} &= \frac{3}{16\pi^2} \left( \frac{\alpha_s}{\pi} \right)^2 \\ &\times \sum_{n \geq 0} \sum_{m=0}^3 \left( \bar{D}_{n,m}^{(2),v}[1] + n_h \bar{D}_{n,m}^{(2),v}[n_h] + n_l \bar{D}_{n,m}^{(2),v}[n_l] \right) z^{-n} \ln^m \frac{-q^2}{m^2}. \end{aligned} \tag{11}$$

In Fig. 2 we show the convergence of the series for the case of the non-diagonal vector correlator. The behavior of the series is shown both for the low-energy and the high-energy expansion. For the high-energy expansion we show the real and the imaginary part. Since the non-diagonal correlators have a cut through three heavy quark lines, the high-energy expansion converges only above  $z = 9$ , which corresponds to a velocity of the heavy quark of  $v = (z - 1)/(z + 1) = 0.8$ .<sup>2</sup> This behavior can also clearly be observed in Tables 2 and 3 which show rapidly growing coefficients corresponding to a radius of convergence  $r < 1$ . Since Table 4 contains only contributions from diagrams with a closed massless-quark loop, the coefficients are better behaved.

---

<sup>2</sup> The diagonal correlators have a four-particle cut starting at three-loops and converge therefore only above  $z = 16$ , i.e.  $v = \sqrt{1 - 1/z} = 0.97$ .

$n$	$\bar{C}_n^{(0),v}$	$\bar{C}_n^{(1),v}$	$\bar{C}_n^{(2),v}[1]$	$\bar{C}_n^{(2),v}[n_h]$	$\bar{C}_n^{(2),v}[n_l]$
1	0.500000	0.457734	-1.51195	0.0166564	0.337837
2	0.133333	-0.0483080	-0.840974	-0.0369934	0.187255
3	0.0555556	-0.115602	-0.665554	-0.0289884	0.135615
4	0.0285714	-0.115219	-0.475376	-0.0213752	0.104474
5	0.0166667	-0.102152	-0.309702	-0.0161172	0.0832408
6	0.0105820	-0.0880811	-0.177592	-0.0125094	0.0679630
7	0.00714286	-0.0756354	-0.0753998	-0.00996452	0.0565728
8	0.00505051	-0.0651894	0.00291844	-0.00811379	0.0478459
9	0.00370370	-0.0565463	0.0628596	-0.00672995	0.0410083
10	0.00279720	-0.0494003	0.108797	-0.00566985	0.0355496
11	0.00216450	-0.0434648	0.144058	-0.00484063	0.0311210
12	0.00170940	-0.0385013	0.171144	-0.00418016	0.0274778
13	0.00137363	-0.0343196	0.191926	-0.00364579	0.0244440
14	0.00112045	-0.0307699	0.207816	-0.00320745	0.0218902
15	0.000925926	-0.0277347	0.219882	-0.00284350	0.0197199
16	0.000773994	-0.0251214	0.228940	-0.00253805	0.0178596
17	0.000653595	-0.0228568	0.235620	-0.00227923	0.0162527
18	0.000556948	-0.0208824	0.240408	-0.00205802	0.0148551
19	0.000478469	-0.0191512	0.243686	-0.00186749	0.0136316
20	0.000414079	-0.0176253	0.245754	-0.00170221	0.0125545
21	0.000360750	-0.0162738	0.246850	-0.00155793	0.0116011
22	0.000316206	-0.0150713	0.247164	-0.00143123	0.0107532
23	0.000278707	-0.0139968	0.246847	-0.00131937	0.00999562
24	0.000246914	-0.0130328	0.246023	-0.00122012	0.00931596
25	0.000219780	-0.0121648	0.244790	-0.00113166	0.00870382
26	0.000196483	-0.0113806	0.243229	-0.00105247	0.00815053
27	0.000176367	-0.0106696	0.241406	-0.000981314	0.00764873
28	0.000158907	-0.0100231	0.239376	-0.000917133	0.00719220
29	0.000143678	-0.00943357	0.237182	-0.000859046	0.00677564
30	0.000130336	-0.00889448	0.234861	-0.000806306	0.00639448

Table 1

Numerical results for the low-energy moments for the non-diagonal vector correlator in the  $\overline{\text{MS}}$  scheme.



$n$	$\bar{D}_{n,0}^{(2),v}[1]$	$\bar{D}_{n,1}^{(2),v}[1]$	$\bar{D}_{n,2}^{(2),v}[1]$	$\bar{D}_{n,3}^{(2),v}[1]$
0	1.78284	-2.64761	1.83333	0
1	-17.7072	25.1337	-16.3333	3.16667
2	-60.1359	47.0000	-8.00000	0
3	-41.3176	-15.4431	16.0772	-3.32442
4	4.27239	-20.8764	5.72599	0.659122
5	7.18683	-11.8251	0.822323	-0.129739
6	0.493132	-5.22086	2.92024	-0.566886
7	-16.8712	-10.5240	9.71602	-0.991008
8	-56.8660	-43.6415	29.4833	-1.70280
9	-164.387	-190.388	94.9042	-2.87364
10	-485.549	-831.419	339.294	-4.95108
11	-1537.17	-3780.76	1357.43	-8.63056
12	-5240.01	-18141.8	6001.46	-15.2756
13	-18953.8	-91894.0	28790.4	-27.3450
14	-70903.6	-488762	147374	-49.4690
15	-264436	$-2.71202 \cdot 10^6$	794591	-90.2629
16	-922552	$-1.56052 \cdot 10^7$	$4.46970 \cdot 10^6$	-165.935
17	$-2.52510 \cdot 10^6$	$-9.26482 \cdot 10^7$	$2.60485 \cdot 10^7$	-306.988
18	-142055	$-5.65199 \cdot 10^8$	$1.56448 \cdot 10^8$	-571.093
19	$8.11996 \cdot 10^7$	$-3.53100 \cdot 10^9$	$9.64408 \cdot 10^8$	-1067.52
20	$9.74537 \cdot 10^8$	$-2.25279 \cdot 10^{10}$	$6.08196 \cdot 10^9$	-2003.91
21	$8.94750 \cdot 10^9$	$-1.46443 \cdot 10^{11}$	$3.91351 \cdot 10^{10}$	-3775.71
22	$7.44796 \cdot 10^{10}$	$-9.68039 \cdot 10^{11}$	$2.56374 \cdot 10^{11}$	-7137.78
23	$5.91860 \cdot 10^{11}$	$-6.49650 \cdot 10^{12}$	$1.70673 \cdot 10^{12}$	-13533.8
24	$4.59022 \cdot 10^{12}$	$-4.41990 \cdot 10^{13}$	$1.15282 \cdot 10^{13}$	-25729.9
25	$3.51344 \cdot 10^{13}$	$-3.04480 \cdot 10^{14}$	$7.88989 \cdot 10^{13}$	-49035.5
26	$2.67074 \cdot 10^{14}$	$-2.12156 \cdot 10^{15}$	$5.46505 \cdot 10^{14}$	-93657.0
27	$2.02372 \cdot 10^{15}$	$-1.49382 \cdot 10^{16}$	$3.82727 \cdot 10^{15}$	-179244
28	$1.53213 \cdot 10^{16}$	$-1.06201 \cdot 10^{17}$	$2.70750 \cdot 10^{16}$	-343676
29	$1.16067 \cdot 10^{17}$	$-7.61776 \cdot 10^{17}$	$1.93326 \cdot 10^{17}$	-660072
30	$8.80664 \cdot 10^{17}$	$-5.50954 \cdot 10^{18}$	$1.39237 \cdot 10^{18}$	$-1.26974 \cdot 10^6$

Table 2

Three-loop coefficients of the high-energy expansion for the non-diagonal vector correlator in the  $\overline{\text{MS}}$  scheme with  $n_h = n_l = 0$ .

$n$	$\bar{D}_{n,0}^{(2),v}[n_h]$	$\bar{D}_{n,1}^{(2),v}[n_h]$	$\bar{D}_{n,2}^{(2),v}[n_h]$	$\bar{D}_{n,3}^{(2),v}[n_h]$
0	-0.251201	0.153727	-0.111111	0
1	0.154182	-1.14726	0.555556	-0.111111
2	3.61746	-1.14459	-0.666667	0
3	1.27971	2.67597	1.06790	0.185185
4	-3.99022	-1.81636	-0.861111	-0.543210
5	-8.59452	0.842895	1.23685	-1.15062
6	-25.2903	-2.26222	8.70815	-1.68560
7	-65.3844	-31.4942	28.2131	-2.18624
8	-164.223	-160.905	86.7525	-2.66878
9	-441.129	-715.641	295.743	-3.14070
10	-1320.45	-3233.48	1154.83	-3.60588
11	-4384.76	-15440.6	5072.08	-4.06652
12	-15690.9	-78173.7	24362.3	-4.52396
13	-58311.1	-416730	125176	-4.97906
14	-215239	$-2.32045 \cdot 10^6$	677824	-5.43239
15	-732644	$-1.34050 \cdot 10^7$	$3.82947 \cdot 10^6$	-5.88438
16	$-1.83932 \cdot 10^6$	$-7.99084 \cdot 10^7$	$2.24126 \cdot 10^7$	-6.33529
17	$1.84847 \cdot 10^6$	$-4.89431 \cdot 10^8$	$1.35168 \cdot 10^8$	-6.78534
18	$8.23216 \cdot 10^7$	$-3.06952 \cdot 10^9$	$8.36569 \cdot 10^8$	-7.23470
19	$9.21471 \cdot 10^8$	$-1.96567 \cdot 10^{10}$	$5.29604 \cdot 10^9$	-7.68348
20	$8.27344 \cdot 10^9$	$-1.28233 \cdot 10^{11}$	$3.42033 \cdot 10^{10}$	-8.13178
21	$6.81847 \cdot 10^{10}$	$-8.50550 \cdot 10^{11}$	$2.24852 \cdot 10^{11}$	-8.57968
22	$5.39132 \cdot 10^{11}$	$-5.72647 \cdot 10^{12}$	$1.50188 \cdot 10^{12}$	-9.02723
23	$4.17068 \cdot 10^{12}$	$-3.90796 \cdot 10^{13}$	$1.01766 \cdot 10^{13}$	-9.47449
24	$3.18860 \cdot 10^{13}$	$-2.69998 \cdot 10^{14}$	$6.98579 \cdot 10^{13}$	-9.92149
25	$2.42300 \cdot 10^{14}$	$-1.88650 \cdot 10^{15}$	$4.85260 \cdot 10^{14}$	-10.3683
26	$1.83633 \cdot 10^{15}$	$-1.33179 \cdot 10^{16}$	$3.40755 \cdot 10^{15}$	-10.8149
27	$1.39098 \cdot 10^{16}$	$-9.49177 \cdot 10^{16}$	$2.41677 \cdot 10^{16}$	-11.2613
28	$1.05453 \cdot 10^{17}$	$-6.82454 \cdot 10^{17}$	$1.72987 \cdot 10^{17}$	-11.7075
29	$8.00841 \cdot 10^{17}$	$-4.94695 \cdot 10^{18}$	$1.24877 \cdot 10^{18}$	-12.1537
30	$6.09583 \cdot 10^{18}$	$-3.61318 \cdot 10^{19}$	$9.08598 \cdot 10^{18}$	-12.5997

Table 3

Three-loop contribution proportional to  $n_h$  to the coefficients of the high-energy expansion for the non-diagonal vector correlator in the  $\overline{\text{MS}}$  scheme.

$n$	$\bar{D}_{n,0}^{(2),v}[n_l]$	$\bar{D}_{n,1}^{(2),v}[n_l]$	$\bar{D}_{n,2}^{(2),v}[n_l]$	$\bar{D}_{n,3}^{(2),v}[n_l]$
0	-0.730175	0.153727	-0.111111	0
1	-0.314922	-1.14726	0.555556	-0.111111
2	0.984271	-1.77778	0	0
3	1.27530	-0.0592818	-0.615226	0.0534979
4	0.544450	0.835905	-0.0709877	-0.0246914
5	0.0510031	0.410862	0.0306790	-0.00740741
6	-0.0437552	0.209240	0.0303704	-0.00329218
7	-0.0561161	0.117605	0.0233371	-0.00176367
8	-0.0503344	0.0722787	0.0177016	-0.00105820
9	-0.0420848	0.0475365	0.0136697	-0.000685871
10	-0.0347091	0.0329283	0.0107911	-0.000470312
11	-0.0287111	0.0237565	0.00869670	-0.000336700
12	-0.0239493	0.0177088	0.00713792	-0.000249408
13	-0.0201760	0.0135592	0.00595223	-0.000189934
14	-0.0171671	0.0106166	0.00503229	-0.000148000
15	-0.0147456	0.00847129	0.00430581	-0.000117578
16	-0.0127769	0.00687002	0.00372304	-0.0000949668
17	-0.0111601	0.00565028	0.00324902	-0.0000778089
18	-0.00981938	0.00470458	0.00285863	-0.0000645526
19	-0.00869741	0.00395987	0.00253355	-0.0000541477
20	-0.00775052	0.00336532	0.00226014	-0.0000458663
21	-0.00694509	0.00288479	0.00202813	-0.0000391926
22	-0.00625501	0.00249212	0.00182965	-0.0000337544
23	-0.00565976	0.00216805	0.00165859	-0.0000292783
24	-0.00514313	0.00189817	0.00151016	-0.0000255604
25	-0.00469214	0.00167159	0.00138059	-0.0000224467
26	-0.00429635	0.00147992	0.00126683	-0.0000198192
27	-0.00394727	0.00131666	0.00116643	-0.0000175864
28	-0.00363797	0.00117672	0.00107740	-0.0000156771
29	-0.00336274	0.00105607	0.000998082	-0.0000140345
30	-0.00311683	0.000951473	0.000927135	-0.0000126137

Table 4

Three-loop contribution proportional to  $n_l$  to the coefficients of the high-energy expansion for the non-diagonal vector correlator in the  $\overline{\text{MS}}$  scheme.

## 4 Conclusion

We have used modern techniques to compute 30 terms in the low-energy expansion of the non-diagonal scalar and vector correlators, matching the already available information on diagonal correlators [21]. Using slightly modified methods we have also obtained 30 coefficients in the high-energy expansion of both non-diagonal and diagonal correlators. Due to multiply massive cuts in some of the contributing diagrams it is expected that the high-energy expansion already breaks down significantly above the physical threshold. Using only the previously available coefficients this behaviour is rather difficult to see. The newly computed coefficients, however, clearly support the presence of such a divergence.

As a final remark it should be noted that the expansion via differential equations used in this publication is rather efficient. This means that it is easy to obtain significantly more terms in the expansions if the need arises.

## Acknowledgments

This work was supported by the Deutsche Forschungsgemeinschaft through the SFB/TR-9 “Computational Particle Physics”. A.M. thanks the Landesgraduiertenförderung for support. We like to thank T. Kasprzik, J.H. Kühn and M. Steinhauser for carefully reading the manuscript.

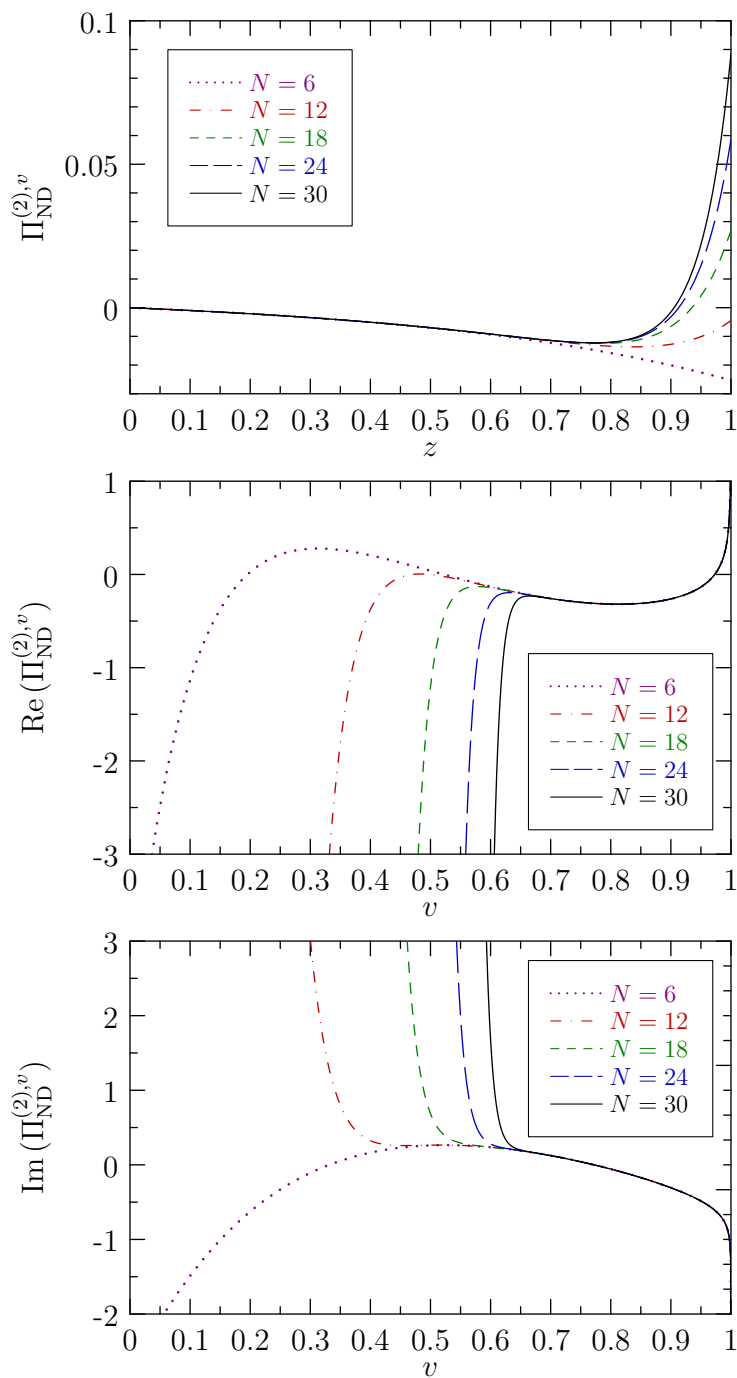


Fig. 2. Convergence of the three-loop contribution to the low- and high-energy expansion of the non-diagonal vector correlator in the  $\overline{\text{MS}}$  scheme for  $n_h = 1$ ,  $n_l = 3$ . The upper figure shows the correlator in the low-energy range for different orders of the expansion in  $z$ . The lower figures show the behavior above threshold for both real and imaginary parts. Note that the high-energy expansion converges only above  $v = 0.8$  which corresponds to the three-particle cut.

## References

- [1] M. A. Shifman, A. I. Vainshtein, V. I. Zakharov. *Nucl. Phys.*, B147:385–447, 1979.
- [2] V. A. Novikov, et al. *Phys. Rept.*, 41:1–133, 1978.
- [3] J. H. Kühn, M. Steinhauser. *Nucl. Phys.*, B619:588–602, 2001.
- [4] R. Boughezal, M. Czakon, T. Schutzmeier. *Phys. Rev.*, D74:074006, 2006.
- [5] J. H. Kühn, M. Steinhauser, C. Sturm. *Nucl. Phys.*, B778:192–215, 2007.
- [6] K. G. Chetyrkin, J. H. Kühn, A. Maier, P. Maierhöfer, P. Marquard, M. Steinhauser, C. Sturm. *Phys. Rev.*, D80:074010, 2009.
- [7] K. Chetyrkin, J. Kühn, A. Maier, P. Maierhofer, P. Marquard, et al. 2010. [arXiv:1010.6157](https://arxiv.org/abs/1010.6157).
- [8] B. Dehnadi, A. H. Hoang, V. Mateu, S. Zebarjad. 2011. [arXiv:1102.2264](https://arxiv.org/abs/1102.2264).
- [9] S. Bodenstein, J. Bordes, C. Dominguez, J. Penarrocha, K. Schilcher. *Phys.Rev.*, D82:114013, 2010.
- [10] I. Allison, et al. *Phys. Rev.*, D78:054513, 2008.
- [11] C. McNeile, C. T. H. Davies, E. Follana, K. Hornbostel, G. P. Lepage. *Phys.Rev.*, D82:034512, 2010.
- [12] A. A. Penin, M. Steinhauser. *Phys. Rev.*, D65:054006, 2002.
- [13] W. Lucha, D. Melikhov, S. Simula. *J.Phys.G*, G38:105002, 2011.
- [14] P. A. Baikov, K. G. Chetyrkin, J. H. Kühn. *Phys. Rev. Lett.*, 101:012002, 2008.
- [15] M. Davier, S. Descotes-Genon, A. Höcker, B. Malaescu, Z. Zhang. *Eur.Phys.J.*, C56:305–322, 2008.
- [16] A. O. G. Källén, A. Sabry. *Kong. Dan. Vid. Sel. Mat. Fys. Med.*, 29N17:1–20, 1955.
- [17] L. Reinders, S. Yazaki, H. Rubinstein. *Phys.Lett.*, B103:63, 1981.
- [18] K. G. Chetyrkin, J. H. Kühn, M. Steinhauser. *Nucl. Phys.*, B505:40–64, 1997.
- [19] K. G. Chetyrkin, M. Steinhauser. *Eur. Phys. J.*, C21:319–338, 2001.
- [20] R. Boughezal, M. Czakon, T. Schutzmeier. *Nucl. Phys. Proc. Suppl.*, 160:160–164, 2006.
- [21] A. Maier, P. Maierhöfer, P. Marquard. *Nucl. Phys.*, B797:218–242, 2008.
- [22] K. G. Chetyrkin, J. H. Kühn, C. Sturm. *Eur. Phys. J.*, C48:107–110, 2006.
- [23] C. Sturm. *JHEP*, 09:075, 2008.

- [24] A. Maier, P. Maierhöfer, P. Marquard. *Phys. Lett.*, B669:88–91, 2008.
- [25] A. Maier, P. Maierhöfer, P. Marquard, A. V. Smirnov. *Nucl. Phys.*, B824:1–18, 2010.
- [26] P. A. Baikov, K. G. Chetyrkin, J. H. Kühn. 2009. [arXiv:0906.2987](#).
- [27] J. Hoff, M. Steinhauser. *Nucl.Phys.*, B849:610–627, 2011.
- [28] K. G. Chetyrkin, J. H. Kühn, M. Steinhauser. *Nucl. Phys.*, B482:213–240, 1996.
- [29] Y. Kiyo, A. Maier, P. Maierhöfer, P. Marquard. *Nucl. Phys.*, B823:269–287, 2009.
- [30] A. H. Hoang, V. Mateu, S. Mohammad Zebarjad. *Nucl. Phys.*, B813:349–369, 2009.
- [31] D. Greynat, S. Peris. *Phys.Rev.*, D82:034030, 2010.
- [32] D. Greynat, P. Masjuan, S. Peris. 2011. [arXiv:1104.3425](#).
- [33] P. Nogueira. *J.Comput.Phys.*, 105:279–289, 1993.
- [34] R. Harlander, T. Seidensticker, M. Steinhauser *Phys. Lett.*, B426:125, 1998; T. Seidensticker [arXiv:hep-ph/9905298](#).
- [35] K. G. Chetyrkin, F. V. Tkachov. *Nucl. Phys.*, B192:159–204, 1981.
- [36] S. Laporta. *Int.J.Mod.Phys.*, A15:5087–5159, 2000.
- [37] P. Marquard, D. Seidel. Unpublished.
- [38] J. Vermaseren. 2000. [arXiv:math-ph/0010025](#).
- [39] A. Kotikov. *Phys.Lett.*, B254:158–164, 1991.
- [40] E. Remiddi. *Nuovo Cim.*, A110:1435–1452, 1997.
- [41] M. Caffo, H. Czyz, S. Laporta, E. Remiddi. *Nuovo Cim.*, A111:365–389, 1998.
- [42] S. Larin. *Phys.Lett.*, B303:113–118, 1993.